

Light Scattering Study of Ionomers in Solution. 5. CONTIN Analysis of Dynamic Scattering Data from Sulfonated Polystyrene Ionomer in a Polar Solvent (Dimethylformamide)

Jeffrey Bodycomb and Masanori Hara*

Department of Mechanics and Materials Science, Rutgers, The State University of New Jersey, Piscataway, New Jersey 08855-0909

Received May 31, 1995; Revised Manuscript Received September 15, 1995[®]

ABSTRACT: Salt-free polyelectrolyte behavior of a random ionomer, partially sulfonated polystyrene (SPS) (Na salt) having an ion content of 2.7 mol %, dissolved in a polar, aprotic solvent, dimethylformamide (DMF), is studied by dynamic light scattering. CONTIN analysis of the data indicates the existence of two diffusive modes, a fast mode and a slow mode. The diffusion coefficient of the fast mode, D_f , on the order of 10^{-6} (cm²/s), increases slightly with ionomer concentration, while the diffusion coefficient of the slow mode, D_s , on the order of 10^{-8} (cm²/s), is independent of ionomer concentration within the concentration range studied. The D_f shows a negative angular dependence, while the D_s shows a positive angular dependence. The fast mode may be explained in terms of the diffusion process enhanced by strong intermolecular electrostatic interactions, and the slow mode may reflect the existence of large-scale "heterogeneities". These conclusions are consistent with those drawn from static (angular) light scattering data for the same system. The results obtained for salt-free ionomers in a polar organic solvent parallel those reported for salt-free polyelectrolytes in water.

Introduction

The behavior of polyelectrolyte solutions with (large amounts of) added salt is rather well understood. Excluded volume theory¹ and scaling theory,² originally developed for understanding the solution behavior of neutral polymers, have been used to explain the behavior of polyelectrolyte solutions with added salts.^{3,4} However, the behavior of polyelectrolytes in salt-free solution (and in solution with very small amounts of added salt) is rather poorly understood.⁴ There still exist controversies about the structure of salt-free solutions and the causes of the characteristic behavior of these solutions. For example, dynamic light scattering has revealed "peculiar" behavior of salt-free polyelectrolyte solutions. It is reported that the effective diffusion coefficient of polyelectrolyte solutions drops precipitously below a certain salt concentration.^{5,6} This so-called *ordinary-extraordinary transition* is now understood in terms of the existence of two diffusion modes, a fast mode and a slow mode; the slow mode dominates at low salt concentrations below a critical salt concentration, which naturally includes salt-free solutions as an extreme case.^{7,8} However, there remains disagreement regarding the interpretation of the two modes, especially that of the slow mode, in the decay of the autocorrelation function of light scattered from salt-free polyelectrolyte solutions.⁷⁻¹⁰ These decay modes in the autocorrelation function are resolved by an inverse Laplace transform and are subject to debate partly due to the inherent difficulty of the problem, particularly when one considers the weak scattering of salt-free polyelectrolyte (aqueous) solutions and the difficulty in optically clarifying aqueous solution. Here, we present dynamic light scattering studies of ionomers in a salt-free, nonaqueous, but polar solvent; such a solution has stronger scattering power and is easier to handle as compared with polyelectrolytes in water.¹¹

Ionomers are a class of ion-containing polymers having a small amount of ionic groups, up to 10–15 mol %,

attached randomly to nonionic backbone chains.¹²⁻¹⁴ In solution, ionomers show two types of behavior depending primarily on the polarity of the solvent:¹⁵ in a low-polarity solvent such as toluene ($\epsilon = 2.4$), *aggregation behavior* due to dipolar attraction is observed, and in a polar solvent, such as dimethylformamide (DMF) ($\epsilon = 37$), *polyelectrolyte behavior* due to Coulombic interactions is observed; ϵ is the dielectric constant of the solvent. Although there have been some reports suggesting aggregate formation even in dilute ionomer solutions in a polar solvent,¹⁶ we think that the behavior observed in a polar solvent (at least in dilute solutions) is generally different from that observed in a low-polarity solvent, which clearly shows aggregate formation. For example, a quite contrasting behavior is seen for viscosity^{15,17} and low-angle light scattering data.^{18,19} The reduced viscosity increases with decreasing polymer concentration in a polar solvent, but decreases in a low-polarity solvent. The reciprocal reduced scattered intensity increases with increasing polymer concentration in a polar solvent, but decreases in a low-polarity solvent. It may be possible, as discussed later, that some aggregation occurs at high ionomer concentrations; but, in dilute solution, we have not noted such evidence. Since much of the work on ionomers has been focused on the structure and properties of solids,¹²⁻¹⁴ the term ionomer is conventionally connected to the aggregation behavior of these materials. In the solid state, ionic groups are dispersed in a medium of low dielectric constant (e.g., ϵ is 2.5 for polyethylene or polystyrene), and counterions are strongly bound to fixed ions; thus the resulting dipolar attraction leads to the formation of ionic aggregates. In this work, however, we will focus our discussion entirely on the *polyelectrolyte behavior* of ionomers in a polar solvent where many of the counterions are dissociated.²⁰ In contrast to solutions of neutral polymers that have relatively weak, short-range interactions on one hand, and polyelectrolytes with almost 100 mol % of ionic groups that have very strong long-range interactions on the other, ionomers are considered to be an intermediate system, which can serve as a good model for investigating the behavior of salt-free polyelectrolyte solutions.^{11,21}

* To whom all correspondence should be addressed.

[®] Abstract published in *Advance ACS Abstracts*, November 1, 1995.

In polar solvents, ionomers show polyelectrolyte behavior in all respects. The reduced viscosity of ionomers increased remarkably with decreasing polymer concentration.^{15,17} This behavior, characteristic of polyelectrolytes, can be suppressed by the addition of simple salts.^{17,20} Low-angle light scattering data from ionomer solutions also show typical polyelectrolyte behavior, i.e., a marked decrease in scattered intensity with increasing polymer concentration (at low concentration range) and ion content.^{18,19} It is of interest to note that telechelic ionomers, with only one or two ionic groups on each polymer chain also show polyelectrolyte behavior observed by viscosity and low-angle light scattering experiments.^{22,23} Small-angle neutron scattering (SANS) and small-angle X-ray scattering (SAXS) on ionomers in a polar solvent also have shown scattering behavior characteristic of polyelectrolytes in aqueous solution:^{16,24,25} a broad single peak in scattered intensity vs scattering vector is observed. All of these observations parallel those from polyelectrolyte/water systems. In addition, dynamic light scattering^{18,26} and osmotic pressure measurements²⁰ for ionomer solutions generally show behavior similar to that of polyelectrolyte solutions. There is a recent review on the behavior of polyelectrolytes and ionomers in nonaqueous solutions.¹¹ It is of interest to note that salt-free polyelectrolyte behavior is observed for ionic polymers irrespective of their ion content, ranging from several mole percent for random ionomers to nearly 100 mol % for polyelectrolytes. However, it should be stressed that the difference in the effective charge density between ionomers and polyelectrolytes is not as great as seemed due to the difference in the degree of counterion binding.²⁷ For example, the osmotic coefficient, ϕ_p , a measure of the fraction of free counterions, is nearly 1.0 for a 3.4 mol % ionomer sample and 0.8 for a 7.3 mol % ionomer sample,²⁰ whereas the value is only 0.2 for 100 mol % poly(styrene sulfonate), polyelectrolyte.²⁸

We have been investigating salt-free polyelectrolyte behavior of ionomers in a polar solvent with various techniques, including viscometry,^{17,29,30} conductimetry,³¹ and static (both low-angle and angular) light scattering.^{19,32} A long-range goal of our work is to extract essential information concerning the "salt-free polyelectrolyte behavior" by using ionomer/nonaqueous solutions. As an ionomer, we use lightly sulfonated polystyrene (SPS) (Na salt). These low charge density polymers (i.e., ionomers) may also be called *weakly charged polyelectrolytes*. However, it should be stressed that SPS ionomers have backbone chains compatible with a polar solvent, e.g., DMF, unlike polyelectrolytes that have backbone chains incompatible with solvent, water. Therefore, neither phase separation nor gelation has been observed for SPS ionomer/DMF systems, as might be expected for weakly charged polyelectrolytes in water.²³

In this work, we extend our previous static scattering studies (the concentration and angular dependence of the static scattering) to include dynamic scattering behavior. Previously, we investigated the dynamic scattering behavior from ionomer solutions, analyzed the results with the method of cumulants, and examined the effect of molecular weight and concentration.²⁶ Although this method may give information of diffusion coefficients, provided that the modes with different diffusion coefficients are well separated and proper use of sample time is made, we can obtain more detailed information by using the Laplace inversion, analyzed

by CONTIN analysis, with a large enough time range. Here, we have conducted dynamic scattering measurements over a broad range of delay times and obtained the spectrum of decay rate by CONTIN analysis. These results confirm the observation that polyelectrolytes in aqueous solution show two separate decay modes in the autocorrelation function and support our contention that ionic polymer systems generally behave similarly in polar solvents.

Experimental Section

Materials. Lightly sulfonated polystyrene (SPS) was made by sulfonation of polystyrene with a sulfonating agent, acetyl sulfate, according to the method reported by Makowski et al.³⁴ The starting polystyrene (PS) had a molecular weight of 400 000 with a narrow molecular weight distribution ($M_w/M_n = 1.06$) (Pressure Chemical). After the sulfonation, acid copolymer samples were recovered by steam stripping, followed by freeze-drying in benzene/methanol (90/10, v/v). Acid copolymers were then converted to ionomer (Na salt) by neutralization in benzene/methanol (90/10, v/v) with methanolic NaOH. The ionomer samples were recovered by freeze-drying, followed by vacuum drying for 1 week. Details about the preparation and characterization of SPS polymers are described elsewhere.^{19,30} The ion content of the ionomer, as determined by titration of acid groups of SPS, was 2.7 mol %; i.e., 2.7 ionic groups per 100 repeat units on average.

Measurements. Polymer stock solutions were prepared by dissolving the freeze-dried ionomer sample in DMF (Fisher: Spectranalyzed grade) under stirring overnight at room temperature. The solutions for the light scattering experiments were made by dilution of the stock solution. Low-angle light scattering experiments were performed with a KMX-6 low-angle light scattering photometer (Chromatix) at a wavelength of 632.8 nm at 25 ± 0.5 °C. The effect of large dust particles was easily removed by using a flow cell. Moreover, since the absolute scattered intensity is directly calculated from the geometrical parameters of the instrument, the usual calibration is unnecessary.³⁵ The specific refractive index increment, dn/dc , was measured at 25 ± 0.1 °C with a KMX-16 differential refractometer (Chromatix). Optical clarification of the solutions was performed by filtration through 0.5 and 0.2 μm filters (Millipore). Details concerning the low-angle light scattering experiments are described elsewhere.¹⁹

Angular light scattering measurements were performed with a Brookhaven BI-200SM photogoniometer (Brookhaven) with a 35 mW He-Ne (632.8 nm) laser light source (Spectraphysics) and a BI-2030 digital correlator (Brookhaven) with 72 data channels, among which 6 delay channels were used for establishing a baseline (infinite time correlation function). Data from the first correlator channel were discarded due to the effects of afterpulsing.³⁶ Each cylindrical cell with 24 mm diameter was cleaned for 2 h with a Thurmond type washing apparatus.³⁷ Then, a cell was mounted at the center of a vat filled with toluene (Fisher: Spectranalyzed grade) to match the refractive index of the glass cell to reduce problems with flare. All measurements were conducted at 25 ± 0.1 °C. Dilution and optical clarification of the solutions were made inside a dust-free hood (Class 100K Hood: Laminare Co.) to avoid contamination by airborne dust. The details concerning the angular light scattering experiments are described elsewhere.³²

After the static scattering measurements, dynamic light scattering experiments were conducted for ionomer solutions over a series of sample times. A correlation function covering a broad range of sample time was obtained by combining experimental curves obtained for four different sample times. For combination, a reference data set was chosen. Then, each of the other three data sets were multiplied by a constant A , unique to each sample time (i.e., shifting curves vertically), such that the sum, $\sum [C_{\text{ref}}(t_i) - AC(t_i)]$, over overlapping delay times, t_i , is minimized, where $C_{\text{ref}}(t_i)$ is the reference correlation function at time t_i and $C(t_i)$ is the measured correlation function to be combined. The composite correlation function was then analyzed by inverse Laplace transformation, ob-

tained by the CONTIN program.³⁸⁻⁴¹ Before combination, data sets were checked for the dust effect by comparing the measured and calculated baselines. When the difference was greater than 0.1%, the data were discarded. An additional check of the dust effect was done by comparing the low-angle (static) scattering data with the angular data extrapolated to zero angle, which was obtained independently, since the dust effect is easily eliminated by using a flow system in KMX-6:³⁵ whenever dust particles enter the scattering volume, spikes are seen in the output signal that records the scattered intensity vs flow time; therefore, by using a baseline value of the recorded output, dust effects on the total scattering are eliminated. The dynamic scattering experiments were conducted at each angle from 30 to 150° in 30° intervals.

Standard Test. To ensure that the appropriate experimental procedure was followed and reasonable data analysis was made, dynamic scattering data were obtained for mixtures of polystyrene standards having different molecular weights (i.e., 50 000 and 400 000). The spectrum of the decay rate obtained by CONTIN analysis produced two distinct peaks corresponding to each PS sample. The diffusion coefficients obtained from the peak positions (or more rigorously the average value $\langle \Gamma \rangle$, where Γ is the decay rate) are 5.8×10^{-7} cm²/s for the 50 000 sample and 1.8×10^{-7} cm²/s for the 400 000 sample. There are in good agreement with the values obtained separately for the individual PS sample. The peak area ratio of the 400 000 sample to the 50 000 sample is 3.4, which is in good agreement with the expected intensity ratio of each peak.

Light Scattering Equations. When the correlation function is deviated from the single exponential function due to the polydispersity of the polymer size or even due to the existence of more than one diffusion mode, dynamic light scattering data may be analyzed by inverse Laplace transformation using the "peak constrained analysis" CONTIN,³⁸⁻⁴¹ this yields a distribution function (spectrum) of decay rate, Γ , $G(\Gamma, q)$, defined by

$$g^{(1)}(q, t) = \int_0^\infty G(\Gamma, q) \exp(-\Gamma t) d\Gamma \quad (1)$$

where $g^{(1)}(q, t)$ is the normalized electric field autocorrelation function at delay time t and scattering vector q . q is defined as $q = (4\pi n_0/\lambda_0) \sin(\theta/2)$, where n_0 is the refractive index of the solvent, λ_0 is the wavelength of the incident light in vacuo, and θ is the scattering angle. Since we usually plot $\log(\Gamma/q^2)$ in an abscissa, eq 1 may be modified as

$$g^{(1)}(q, t) = \int_{-\infty}^\infty \Gamma G(\Gamma, q) \exp(-\Gamma t) d \log(\Gamma/q^2) \quad (2)$$

Equation 2 indicates that when $\Gamma G(\Gamma, q)$ is plotted in an ordinate and $\log(\Gamma/q^2)$ is plotted in an abscissa, the area under the each peak corresponds to the weight of each peak.

Experimentally, the normalized intensity autocorrelation function, $g^{(2)}(q, t)$, is measured first, which can then be converted to the electric field autocorrelation function, $g^{(1)}(q, t)$, via the following Siegert relationship:⁴²⁻⁴⁴

$$g^{(2)}(q, t) = B \{1 + b |g^{(1)}(q, t)|^2\} \quad (3)$$

where B is the (infinite time) baseline and b is an optical constant. The value of B is obtained from the long time delay channels of the composite correlation function.

In the case of simple diffusion, the angular dependence of the decay rate is described by $\Gamma/q^2 = D$, where D is the diffusion coefficient of the polymer.^{43,44} For a more general case, data are interpreted in terms of an effective diffusion coefficient, D_{eff} , which is defined by $D_{\text{eff}} = \langle \Gamma \rangle / q^2$, where $\langle \Gamma \rangle$ is the average value of Γ .

The (mutual) diffusion coefficient of nonaggregating polymer solutions is given by the generalized Stokes-Einstein relation,^{1,45,46}

$$D = \frac{M(1 - \nu c)}{N_A f(c)} (\partial \Pi / \partial c) \quad (4)$$

where M is the molecular weight of the polymer, N_A is Avogadro's number, c is the polymer concentration (g/cm³), $\partial \Pi / \partial c$ is the inverse osmotic compressibility, $f(c)$ is the frictional coefficient of the molecule, and ν is the partial specific volume of the polymer. Strongly interacting systems, such as salt-free polyelectrolyte solutions, show a strong concentration dependence at low concentrations, the major contribution of which comes from the $\partial \Pi / \partial c$ term.²⁶

Since some static scattering data are also obtained and used for discussion, some of the basic equations are summarized here. From fluctuation theory, it is shown that the reciprocal scattered intensity at zero angle can be written in terms of $\partial \Pi / \partial c$ as¹

$$\frac{Kc}{R_0} = \frac{1}{RT} (\partial \Pi / \partial c) \quad (5)$$

where R_0 is the excess reduced scattered intensity at zero angle, R is the gas constant, T is the absolute temperature, and K is the optical constant, defined by $4\pi^2 n_0^2 (dn/dc)^2 / N_A \lambda_0^4$, for vertically polarized incident light, where dn/dc is the refractive index increment. It should be stressed that eq 5 is still applicable to salt-free solutions at $\theta = 0^\circ$, although the equation derived from the fluctuation theory cannot be used at finite angles for such solutions.⁴⁷ Comparison of eqs 4 and 5 indicates that the concentration dependence of D and Kc/R_0 for strongly interacting systems are roughly parallel, since the $\partial \Pi / \partial c$ term is dominant in concentration dependence.⁴⁹

At zero angle, it is also shown³² that

$$\frac{Kc}{R_0} = \frac{1}{M} \left(1 + \frac{N}{V} m_0 \right) \quad (6)$$

where m_0 is the intermolecular excluded volume and N is the number of molecules in the scattering volume, V . Thus, Kc/R_0 is used as a measure of intermolecular excluded volume (see eq 6), as well as the inverse osmotic compressibility, $\partial \Pi / \partial c$ (see eq 5).

Angular dependence of static light scattering data for strongly interacting systems has been considered in a previous paper.³² Reciprocal reduced scattered intensity, Kc/R_θ , may be written as

$$\frac{Kc}{R_\theta} = \left(\frac{Kc}{R_0} \right) \left[1 + q^2 \left\{ \frac{R_g^2}{3} - \frac{\xi^2}{6} \left(1 - \frac{R_0}{MKc} \right) \right\} - C' q^4 \right] \quad (7)$$

where R_θ is the excess reduced scattered intensity at angle θ , R_g is the radius of gyration of the scatterer, ξ is the root-mean-square radius of the intermolecular excluded volume (exclusion zone), and C' is a constant. The coefficient of the q^2 term in eq 7 is considered to be the apparent radius of gyration, $R_{g,\text{app}}$:

$$\frac{R_{g,\text{app}}^2}{3} = \frac{R_g^2}{3} - \frac{\xi^2}{6} \left(1 - \frac{R_0}{MKc} \right) \quad (8)$$

Equation 8 indicates that the initial slope of the angular-dependent curves in a Zimm plot is determined by two competing terms: one is the first term including R_g^2 that reflects the radius of gyration of the polyion chains (a positive contribution), and the other is the second term including ξ^2 that reflects the intermolecular excluded volume (a negative contribution).

When both the (static) intensity data, R_θ , and (dynamic) CONTIN data are available, we may estimate the contribution from each mode, determined by the peak area for each mode in the spectrum of Γ . If the weight of the spectrum is proportional to the scattered intensity from the each mode,⁵² as typically seen for dilute neutral polymer solutions (e.g., a mixture of polymers with two different molecular weights), the scattering contribution of the each mode may be obtained from the following relation:

$$R_{\theta,i} = R_\theta \frac{\int_{\text{peak } i} G(\Gamma, q) d\Gamma}{\int_{\text{all peaks}} G(\Gamma, q) d\Gamma} \quad (9)$$

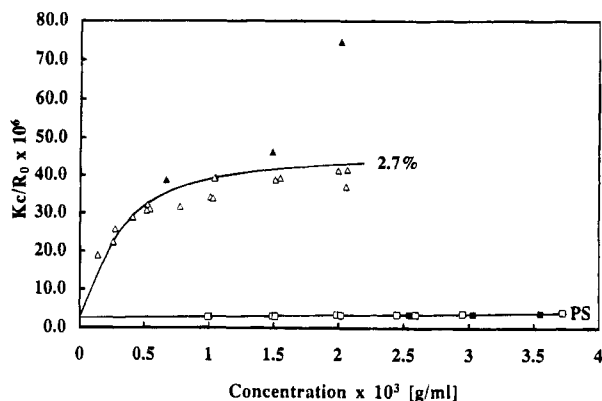


Figure 1. Low-angle light scattering data (closed symbols) and wide-angle data extrapolated to zero angle (open symbols) for the ionomer as well as for PS in DMF.

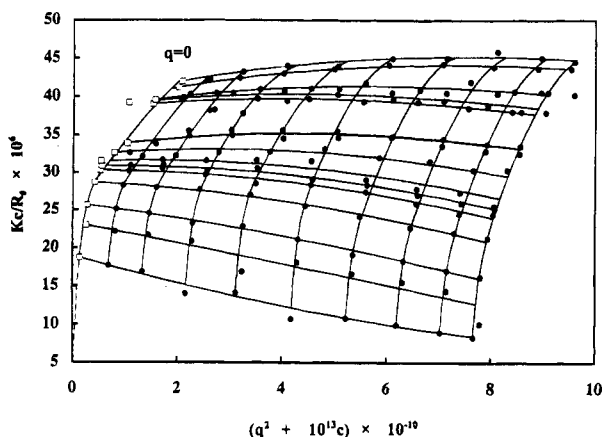


Figure 2. Zimm plot of the ionomer in DMF.

where $R_{\theta,i}$ is the scattering from the i th mode of the spectrum. As part of the standard test, this equation was used to separate the contribution of each PS in a PS mixture (50 000 and 400 000). We could obtain reasonable R_g values from the angular dependence of reciprocal scattered intensity, $1/R_{\theta,i}$.

Results

Figure 1 shows low-angle light scattering data as well as the angular data, extrapolated to zero angle, for the ionomer having an ion content of 2.7 mol % in DMF and for the parent polystyrene. The reciprocal reduced scattered intensity, Kc/R_0 , rises steeply from the intercept at zero concentration, bends over, and becomes nearly horizontal at higher concentrations with a final value much larger than that of the unmodified polystyrene. This is interpreted as arising from a large inverse osmotic compressibility term, $(\partial\Pi/\partial c)$, in a thermodynamic sense (see eq 5) or from a large intermolecular excluded volume term (see eq 6). This behavior is in agreement with the results reported on random ionomers in a polar solvent^{18,19} and polyelectrolytes in aqueous solution.^{51,53}

Figure 2 shows a Zimm plot obtained from angular measurements for the ionomer solution. The most significant point of the figure is the negative angular dependence of Kc/R_0 at low polymer concentrations and the positive angular dependence at higher polymer concentrations. This has been interpreted in terms of the intermolecular excluded volume (of the repulsion zone) dominant at low concentrations (ξ^2 term in eq 8) and large-scale "heterogeneities" dominant at high concentrations (R_g term in eq 8), as discussed in detail in a previous paper.³² For salt-free polyion solutions

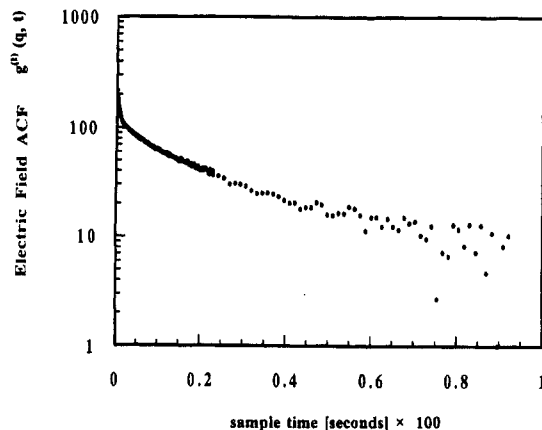


Figure 3. Decay of the electric field autocorrelation function, $g^{(1)}(q,t)$, for the ionomer in DMF. Note log scale.

at low concentrations (except at extremely low concentrations⁵⁴), ξ is much larger than R_g due to the presence of the large exclusion zone brought about by the electrostatic interactions and the $(1 - R_0/MKc)$ term in eq 8 is close to 1 (as seen in Figure 1); thus, the negative contribution is dominant and the initial slope of the angular-dependent curves is negative. In contrast, at higher concentrations, since R_g and ξ become comparable and the $(1 - R_0/MKc)$ term is close to 1, the positive term becomes important and the apparent radius of gyration is reduced due to the ξ^2 term. This effect is small in the case of neutral polymers with weak intermolecular interactions. However, in the case of ionic polymers with strong intermolecular interactions, the ξ^2 term is overwhelming at low concentrations.³²

To further understand the characteristic salt-free behavior of ionomer solutions, dynamic light scattering studies were conducted. Since the flow cell system of the KMX-6 low-angle light scattering instrument allows us to remove the scattering contribution from large dust particles, the angular data extrapolated to 0° were compared with those from low-angle measurements to ensure that the angular data were free from the dust effect and thus reliable for further analysis.³² After the angular measurements, dynamic light scattering measurements were conducted for the same sample cell.

Figure 3 shows the decay of the autocorrelation function for an SPS ionomer sample in DMF. The figure indicates that the scattering data cannot be described by a single exponential function (otherwise the data would follow a straight line). The deviation from the single exponential function has been pointed out before for random ionomer solutions.²⁶

Figure 4 shows distributions (spectrum) of the decay rate for the ionomer as well as for unmodified PS, analyzed with the CONTIN program.³⁸⁻⁴¹ The figure shows at least two distinct peaks over a wide range of time scales for the ionomer solution, in contrast to the unmodified PS solution, which shows only a single peak. In some cases, the analysis of the scattering data indicated the presence of a third relaxation mode (see Figure 5). Since the bulk of the data have consistently indicated two scattering modes, all data were analyzed in such a way to force the data interpretation in terms of two peaks or less, allowing us to account for all of the scattering from the solution. The (weighted) average decay rate, $\langle\Gamma\rangle$, i.e., the first moment of $G(\Gamma,q)$ divided by the zeroth moment of $G(\Gamma,q)$, was taken as the peak position. It should be added that the Laplace inversion is a delicate process due to ill-conditioned

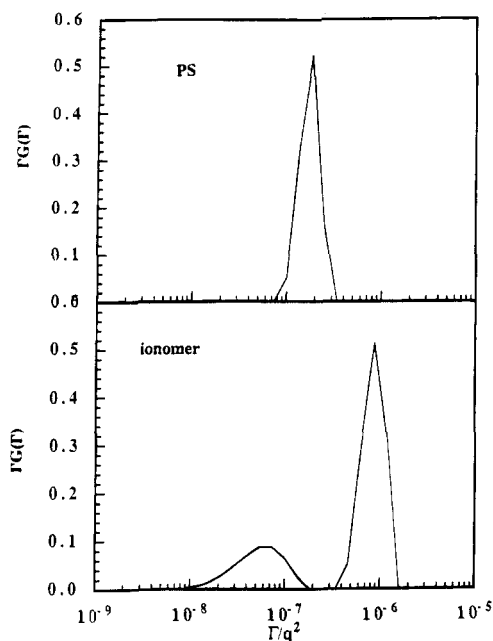


Figure 4. Spectrum of decay rate, Γ , normalized by q^2 , of dynamic light scattering data, analyzed by CONTIN ($\theta = 60^\circ$), for the ionomer as well as for PS in DMF.

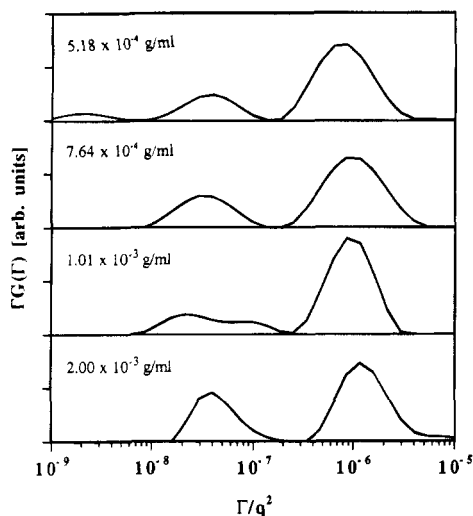


Figure 5. Spectrum of decay rate, Γ , normalized by q^2 , of dynamic light scattering data, analyzed by CONTIN ($\theta = 90^\circ$), for the ionomer in DMF at different ionomer concentrations.

problems involved, so that care must be exercised in extracting information.⁵²

Figure 6 shows the q^2 dependence of $\langle \Gamma \rangle / q^2$, the average decay rate over q^2 , for the ionomer as well as for unmodified PS. For simplicity, a line is drawn for the data obtained at one concentration by using a least-squares method. A similar procedure is applied to all the data obtained at different concentrations. As observed for polyelectrolytes in aqueous solution, some deviation from the diffusive relation, $\langle \Gamma \rangle \propto q^2$, is noted.⁷⁻⁹ The fast mode ($\langle \Gamma_f \rangle / q^2 = D_{\text{eff},f} \sim 10^{-6} \text{ cm}^2/\text{s}$) shows a very slightly negative q^2 dependence, while the slow mode ($\langle \Gamma_s \rangle / q^2 = D_{\text{eff},s} \sim 10^{-8} \text{ cm}^2/\text{s}$) shows a slightly positive q^2 dependence. The negative slope of D_f^0 and the positive slope of D_s^0 were also reported for salt-free polyelectrolyte solutions. Due to the preliminary nature of the data, we will not examine in detail the q^2 dependence of the fast mode and the slow mode.

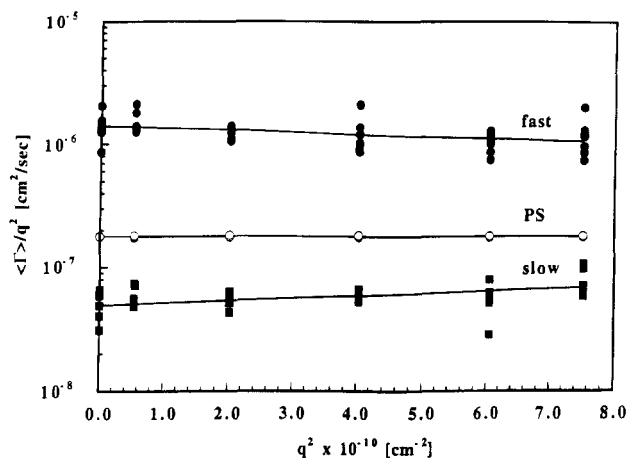


Figure 6. Average Γ value normalized by q^2 , $\langle \Gamma \rangle / q^2$, as a function of q^2 for the ionomer in DMF: (●) fast mode; (■) slow mode. Also shown are the data for PS in DMF (○).

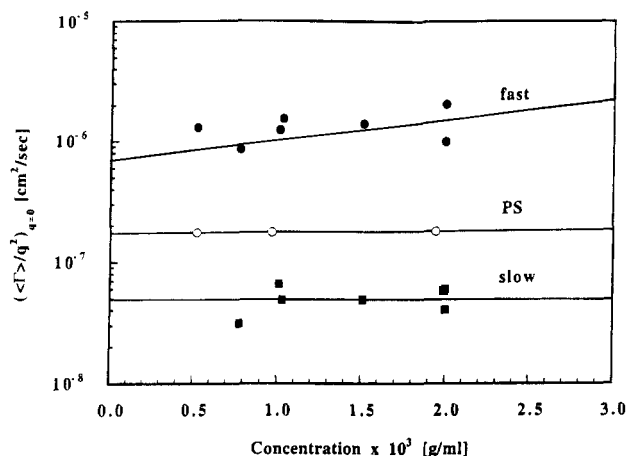


Figure 7. Average peak position extrapolated to $q = 0$, $[\langle \Gamma \rangle / q^2]_{q=0}$, as a function of polymer concentration for the ionomer in DMF: (●) fast mode; (■) slow mode. Also shown are the data for PS in DMF (○).

To examine the concentration dependence, a limiting value of $\langle \Gamma \rangle / q^2$ at $q = 0$, $(\langle \Gamma \rangle / q^2)_{q=0}$, which was obtained as the intercept of the lines in Figure 6, is plotted as a function of polymer concentration in Figure 7. There is a slight increase in $(\langle \Gamma \rangle / q^2)_{q=0}$ ($=D_f^0$) value with concentration for the fast mode, but no discernible concentration dependence is noted for the slow mode (D_s^0). The concentration dependence of the fast mode may be compared with the concentration dependence of Kc/R_0 in Figure 1. A log-scale plot of Kc/R_0 is shown in Figure 8 for comparison. Over the concentration range studied by dynamic light scattering, i.e., $(0.5-2) \times 10^{-3} \text{ g/cm}^3$, a slight increase in the log plot should be observed, as seen from Figure 8 and predicted from eqs 4 and 5: this is because Kc/R_0 is proportional to $\partial \Pi / \partial c$ (see eq 5), and the mutual diffusion coefficient, D , is also proportional to $\partial \Pi / \partial c$ for strongly interacting polymer solutions (see eq 4). A more significant increase in D_f^0 with polymer concentration was reported for polyelectrolyte solutions.^{7,8} While it has been observed that D_s^0 changes significantly with concentration for salt-free polyelectrolyte solutions, no such behavior is noted for the ionomer samples studied. This may be because the ion content (therefore, electrostatic interactions) is low and a relatively narrow concentration range is covered in this work.

Figure 9 gives the reciprocal of the calculated scattered intensities from the each mode by using eq 9. The

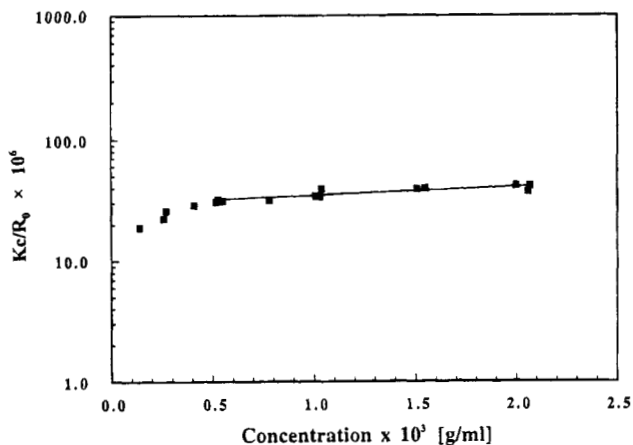


Figure 8. Low-angle light scattering data for the ionomer in DMF, where the ordinate is plotted in a log scale.

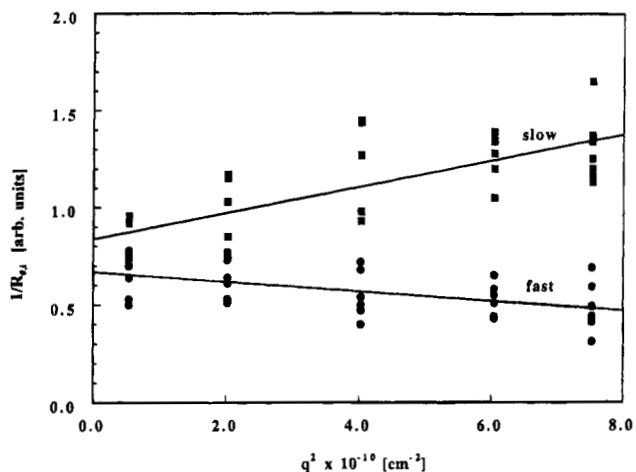


Figure 9. Inverse scattered intensity of each peak ($1/R_{\theta,i}$ vs q^2) for the ionomer in DMF: (●) fast mode; (■) slow mode. Note that concentration effects are ignored for drawing lines.

figure indicates that the fast mode peak shows a negative q^2 dependence in its reciprocal scattered intensity, whereas the slow mode shows a positive q^2 dependence, which is consistent with the static scattering data, as will be discussed later. It should be stressed that the cross terms involved in the derivation of the dynamic structure factor cannot be taken to be zero for strongly interacting systems (e.g., polyion solutions) due to the correlations between different polymers, unlike for a weakly interacting system (e.g., dilute neutral polymer solutions).⁵² Since these are the necessary conditions for using eq 9, we only used the relationship to qualitatively discuss the angular dependence for the ionomer solution.

Discussion

Two Modes. Our CONTIN analysis of the decay rate for ionomer dilute solutions in a polar solvent clearly indicates the existence of *two decay modes* (a fast mode and a slow mode). Both modes basically show q^2 dependence; therefore they are diffusive processes. This behavior is similar to that observed for salt-free polyelectrolytes in aqueous solution.^{7,8}

The *fast (diffusive) mode* may be interpreted as arising from polyion-counterion coupling, in which fast moving counterions “drag” slow moving polyions, leading to larger diffusion coefficients of polyions; under salt-free conditions, the diffusion coefficient can be shown to approach that of the small ions,⁴³ and thus the five-

fold increase in the diffusion coefficient of single ionomer chains as compared with PS (as seen in Figures 6 and 7) is not unreasonable. Alternatively, and more generally, the fast mode may be interpreted in terms of nonequilibrium thermodynamics: diffusion is caused by the “thermodynamic driving force” for diffusion, i.e., chemical potential gradient, which is proportional to the inverse osmotic compressibility, $\partial\Pi/\partial c$, as seen in the generalized Stokes–Einstein relation (eq 4). Since the $\partial\Pi/\partial c$ value is very large for polyion solutions, arising from the large intermolecular excluded volume term, $(N/V)m_0$, due to repulsive interactions (see eq 6), the diffusion coefficients of polyions are significantly enhanced. In fact, as seen in Figure 1, there is a 10 times increase in Kc/R_0 value as compared with PS. In addition, the reciprocal scattering of the fast mode shows a negative angular dependence (see Figure 9), which is consistent with the results obtained by static scattering of ionomers in a polar solvent at low concentrations where the fast mode is dominant (see Figure 2); at low ionomer concentrations, Zimm plots of ionomers in a polar solvent show negative slopes, which are explained as arising from external interference due to strong electrostatic interactions between polyions.³² Therefore, it seems that low concentration data of both static and dynamic scattering are consistently explained in terms of *intermolecular (electrostatic) interactions*.

The *slow (diffusive) mode*, whose diffusion coefficient is 1–2 orders of magnitude lower than that of the fast mode, may be interpreted as arising from the presence of large-scale “heterogeneities”. The diffusion coefficient of the slow mode, D_s , is 5×10^{-8} cm²/s for the ionomer solution (as seen in Figure 7). This corresponds to a hydrodynamic radius, R_h , of 475 Å, 3.6 times that of the unmodified PS, 130 Å (with a diffusion coefficient of 1.8×10^{-7} cm²/s). Here, the Stokes–Einstein relation ($D = kT/6\pi\eta R_h$) is used to evaluate the R_h value, where k is the Boltzmann constant and η is the viscosity of the solution.⁴³ In addition, the reciprocal scattering of the slow mode (Figure 9) leads to an apparent radius of gyration, $R_{g,app}$, of ca. 500 Å, twice that of the parent polystyrene (239 Å). Clearly, these values disagree quantitatively; however, it should be emphasized that the radius of gyration is modified by intermolecular interactions, i.e., the ξ^2 term in eq 8, which tend to reduce the $R_{g,app}$ value. From static (angular) measurements of SPS ionomer solution in DMF, we have observed that the slopes of angular-dependent curves in the Zimm plot increase with ionomer concentration, from initially negative values at low concentrations to large positive values at higher ionomer concentrations (see Figure 2). The apparent radius of gyration of ca. 300 Å, obtained at high concentrations, is smaller than the 500 Å obtained from the slope of the slow mode (in Figure 9), because in a Zimm plot the effects of both fast and slow modes are involved and a negative contribution from the fast mode decreases the overall slope. The large value of $R_{g,app}$ for the ionomer solution as compared with PS was previously interpreted as evidence of large-scale “heterogeneities” existing in the ionomer solution.³² Therefore, it seems that the high concentration data of both static and dynamic scatterings are consistently explained in terms of large-scale “heterogeneities” existing in solution.

Somewhat similar dynamic light scattering behavior was reported for salt-free polyelectrolyte solutions, sodium poly(styrenesulfonate)⁷ and quaternized PVP⁸ in water. These results, coupled with some static light

scattering results, have been interpreted as arising from large-scale "domains" in the solution.⁹ Some explanations have been proposed to explain the formation of such "domains" in salt-free polyion solutions. One explanation is offered by Ise et al.⁵⁵ They attributed the origin of such behavior to attractive interaction between different polyions through intermediary counterions with opposite sign. In their "two-state model", both free polyions and associated species (corresponding to the "domain") coexist in the solution. Another is the so-called "temporal aggregate" model by Schmitz et al.,⁵ which explains the formation of "domains" due to dipole-dipole type attractions through the distortion of ion clouds. However, there are some arguments against the existence of "domains".¹⁰ It should also be added that even neutral polymer solutions (especially semidilute solutions) show somewhat similar dynamic light scattering results at high concentrations.^{52,56,57} Certainly, no attraction due to ionic interactions is expected for the neutral polymer solutions. It is not our intention in this paper, however, to identify the origin of "heterogeneities" found in salt-free ionomer solutions. More systematic studies to characterize the "heterogeneities" and experiments targeted to separate the essential factors causing the behavior are needed. Further studies will address these issues. Nevertheless, we have clearly shown characteristic dynamic light scattering behavior of salt-free ionomer solutions in a polar solvent, such as the appearance of the slow mode in addition to the fast mode, which are consistent with results obtained by dynamic light scattering on salt-free polyelectrolyte solutions.

Comparison with Previous Results. The results obtained by CONTIN analysis should be compared with those obtained previously by the method of cumulants for SPS ionomer solutions.²⁶ It was shown that for high molecular weight ionomers (MW: 200 000 and 400 000), the effective diffusion coefficient, D_{eff} , obtained from the first cumulant by using the $D_{\text{eff}} = \langle \Gamma \rangle / q^2$ relation, increases significantly with ionomer concentration and bends over at high ionomer concentration. It is also noted that the D_{eff} value increases with ion content of the ionomers at fixed polymer concentrations. We have pointed out that the results are consistent with those found for the same ionomers by low-angle light scattering: i.e., the reciprocal reduced scattered intensity increases significantly with ionomer concentration, becomes almost horizontal at higher concentration, and at a fixed ionomer concentration, increases with ion content (see eqs 4 and 5). As already discussed above, these results reflect a significant increase in inverse osmotic compressibility with polymer concentration, which arises from long-range electrostatic interactions among ionomer molecules in salt-free solution. By comparing with our present results by CONTIN, this behavior seems to correspond to that of the fast mode.

In contrast, for a low molecular weight ionomer (MW: 50 000), quite contrasting dynamic behavior is observed: the D_{eff} is insensitive to ionomer concentration, and at a fixed polymer concentration, the D_{eff} decreases with ion content. A similar concentration and ion content dependence was also reported for the SPS ionomer (MW: 100 000) in DMF, obtained by a forced single exponential fit.¹⁸ Again, by comparing with our current results by CONTIN, this behavior seems to correspond to that of the slow mode.

In dynamic light scattering experiments conducted initially for ionomer solutions,¹⁸ including our previous

work,²⁶ sample times were set to be in a relatively narrow range; especially, a large channel (sample) time, needed to cover the slow mode of large (high molecular weight) ionomers, was not used. Therefore, it is likely that, under the similar (normal) sample time range used, only the fast diffusion mode was detected for high molecular weight (i.e., large) ionomers, while only the slow diffusion mode was detected for low molecular weight (i.e., small) ionomers.

This assessment is supported by the observation which indicates a marked channel time dependence of D_{eff} obtained by the method of cumulants for DNA solution. At low salt concentration, the DNA solution is in an "extraordinary" regime where the slow mode is dominant. For example, at a salt concentration of 0.0025 M and a DNA concentration of 8.5×10^{-3} g/cm³, a short channel time (0.5–4 μ s) led to a D_{eff} of 9×10^{-7} cm²/s, while a long channel time (6–60 μ s) led to a D_{eff} of 2×10^{-7} cm²/s. This result has been explained as arising from the presence of two diffusion modes;⁵⁸ a short channel time covers the fast mode, while a large channel time covers the slow mode. Moreover, the data indicated a sharp increase in D_f with polymer (DNA) concentration, while the D_s was almost independent of polymer concentration. The former behavior is consistent with our results by the method of cumulants observed for high MW ionomer samples (Figures 3 and 4 of ref 26a), and the latter behavior is consistent with that observed for a low MW ionomer sample (Figure 5 of ref 26a). Also, our current data by CONTIN (Figure 7) indicate the same behavior for both the fast mode and the slow mode, except that a sharp increase in D_f at low concentration is not seen because of the lack of very low concentration data. (However, we should observe such behavior, judging from the comparison between Figures 7 and 8, as already discussed.) It is also reported for salt-free sodium poly(styrenesulfonate) (PSS) solution that little dependence of D_s on the polyion concentration was detected for low MW samples ($< 10^5$), although a large dependence (up to 2 orders) is seen for higher MW samples ($> 10^5$).^{7,59} Therefore, the slow mode seen for the low MW ionomer sample (Figure 5 of ref 26a) is consistent with the PSS results.

In short, the previous results obtained by the method of cumulants are consistent with the present results obtained by CONTIN, and apparently contrasting behavior for high and low molecular weight ionomers arises from the observation of the different mode (one mode only) in the previous study. These results indicate the more general usefulness of CONTIN analysis of the dynamic light scattering data to obtain detailed information concerning the dynamic behavior and structure of ionomer solutions.

Conclusions

Two diffusive modes (a fast mode and a slow mode) have been identified for random ionomers having an ion content of 2.7 mol %, dissolved in a polar solvent, DMF. Two modes have diffusion coefficients with values differing by 2 orders of magnitude. The diffusion coefficient of the fast mode increases slightly with polymer concentration, which is in accord with the low-angle static scattering data. The reciprocal scattered intensity obtained from the fast mode also shows a negative angular dependence, which is consistent with the angular dependence of static scattering data at low polymer concentrations. The behavior is explained consistently in terms of the large inverse osmotic com-

compressibility due to the large intermolecular excluded volume of the system. The diffusion coefficient of the slow mode is independent of polymer concentration over the concentration range studied (which is rather narrow compared with some dynamic scattering studies reported for salt-free polyelectrolyte solutions). The reciprocal scattered intensity obtained from the slow mode is also consistent with the angular dependence of static scattering data at high polymer concentrations; i.e., large positive slopes, leading to larger $R_{g,app}$ as compared with that of the single polymer chain, are noted. This seems to reflect the existence of large-scale "heterogeneities", whose origin, nature, and structures are currently controversial. Previous results obtained by the method of cumulants, which shows contrasting behavior for high and low molecular weight ionomer samples, can now be understood in terms of the detection of only one mode under the experimental conditions used.

Dynamic behavior of (random) ionomer solutions is found to be essentially similar to that of salt-free polyelectrolyte solutions, as already noted for viscosity, static (low-angle and angular) light scattering, and small-angle X-ray and neutron scatterings. It is especially of interest to note that random ionomers used for solution studies have typically ionic groups of only several mole percent in contrast to nearly 100 mol % in polyelectrolytes. Therefore, it seems that salt-free polyelectrolyte behavior is seen for ionic polymers (dissolved in a polar solvent) irrespective of their charge density, although the lower limit of ion content for producing polyelectrolyte behavior needs to be fully investigated. Such studies can be done by using random ionomers having extremely small ion contents (e.g., less than 1 mol %) and, more ideally, monotelechelic ionomers (which have only one ionic group per chain). These studies are currently underway in this laboratory and will be reported.

Acknowledgment is made to the Petroleum Research Fund, administered by the American Chemical Society, for support of this research. We thank G. Kupperblatt for his technical assistance and preparation of figures.

References and Notes

- (1) Yamakawa, H. *Modern Theory of Polymer Solutions*; Harper and Row: New York, 1971.
- (2) de Gennes, P.-G. *Scaling Concepts in Polymer Physics*; Cornell University Press: Ithaca, NY, 1979.
- (3) Nagasawa, M.; Takahashi, A. In *Light Scattering from Polymer Solutions*; Huglin, M. B., Ed.; Academic Press: New York, 1972; Chapter 16.
- (4) Mandel, M. In *Polyelectrolytes: Science and Technology*; Hara, M., Ed.; Marcel Dekker: New York, 1993; Chapter 1.
- (5) Schmitz, K. S.; Lu, M.; Gauntt, J. *J. Chem. Phys.* **1983**, *78*, 5059.
- (6) Amis, E. In *Polyelectrolytes: Science and Technology*; Hara, M., Ed.; Marcel Dekker: New York, 1993; Chapter 3 (see also references therein).
- (7) Sedlak, M.; Amis, E. *J. Chem. Phys.* **1992**, *96*, 826; **1992**, *96*, 817.
- (8) Förster, S.; Schmidt, M.; Antonietti, M. *Polymer* **1990**, *31*, 781.
- (9) Sedlak, M. *Macromolecules* **1993**, *26*, 1158.
- (10) Li, X.; Reed, W. F. *J. Chem. Phys.* **1991**, *94*, 4568.
- (11) Hara, M. In *Polyelectrolytes: Science and Technology*; Hara, M., Ed.; Marcel Dekker: New York, 1993; Chapter 4.
- (12) Holliday, L., Ed. *Ionic Polymers*; Applied Science: London, 1975.
- (13) Eisenberg, A.; King, M. *Ion Containing Polymers*; Academic: New York, 1977.
- (14) MacKnight, W. J.; Earnest, T. R. *J. Polym. Sci., Macromol. Rev.* **1981**, *16*, 41.
- (15) Lundberg, R. D.; Phillips, R. R. *J. Polym. Sci., Polym. Phys. Ed.* **1982**, *20*, 1143.
- (16) Wang, J.; Wang, Z.; Peiffer, D. G.; Shuely, W. J.; Chu, B. *Macromolecules* **1991**, *24*, 790.
- (17) Hara, M.; Wu, J.; Lee, A. H. *Macromolecules* **1989**, *22*, 754.
- (18) Lantman, C. W.; MacKnight, W. J.; Peiffer, D. G.; Sinha, S. K.; Lundberg, R. D. *Macromolecules* **1987**, *20*, 1096.
- (19) Hara, M.; Wu, J. *Macromolecules* **1988**, *21*, 402; **1986**, *19*, 2887.
- (20) Rochas, C.; Domard, A.; Rinaudo, M. *Polymer* **1979**, *20*, 76.
- (21) Weill, G. *Biophys. Chem.* **1991**, *41*, 1.
- (22) Hara, M.; Wu, J.; Jerome, R. J.; Granville, M. *Macromolecules* **1988**, *21*, 3330.
- (23) Wu, J.; Wang, Y.; Hara, M.; Granville, M.; Jerome, R. *Macromolecules* **1994**, *27*, 1195.
- (24) Lantman, C. W.; MacKnight, W. J.; Sinha, S. K.; Peiffer, D. G.; Lundberg, R. D.; Wignall, G. D. *Macromolecules* **1988**, *19*, 1344.
- (25) Aldebert, P.; Dreyfus, B.; Pineri, M. *Macromolecules* **1986**, *19*, 2651.
- (26) (a) Wu, J.; Hara, M. *Macromolecules* **1994**, *27*, 923. (b) Hara, M.; Wu, J. *ACS Symp. Ser.* **1989**, *395*, 446.
- (27) Manning, G. S. *Annu. Rev. Phys. Chem.* **1972**, *23*, 117.
- (28) Takahashi, A.; Kato, N.; Nagasawa, M. *J. Phys. Chem.* **1970**, *74*, 944.
- (29) Hara, M.; Wu, J.; Lee, A. H. *Macromolecules* **1988**, *21*, 2214.
- (30) Hara, M.; Lee, A. H.; Wu, J. *J. Polym. Sci., Polym. Phys. Ed.* **1987**, *25*, 1407.
- (31) Kupperblatt, G.; Hara, M. *Macromolecules*, to be submitted for publication.
- (32) Bodycomb, J.; Hara, M. *Macromolecules* **1994**, *27*, 7369.
- (33) Borue, V. Y.; Erukhimovich, I. Y. *Macromolecules* **1988**, *21*, 3240.
- (34) Makowski, H. S.; Lundberg, R. D.; Singhal, G. H. U.S. Patent 3870841, 1975 (assigned to Exxon Research and Engineering Co.).
- (35) Kaye, W.; McDaniel, J. B. *J. Appl. Opt.* **1973**, *12*, 541.
- (36) Instruction Manual for BI-2030 Digital Correlator.
- (37) Thurmond, C. D. *J. Polym. Sci.* **1952**, *8*, 607.
- (38) Provencher, S. W.; Hendrix, J.; Maeyer, L. D. *J. Chem. Phys.* **1978**, *69*, 4273.
- (39) Provencher, S. W. *Makromol. Chem.* **1979**, *180*, 201.
- (40) Provencher, S. W. *Comput. Phys. Comm.* **1982**, *27*, 213; **1982**, *27*, 229.
- (41) Provencher, S. W. *Contin (Version 2) Users Manual*. Technical Report; Max Planck Institut für Biophysikalische Chemie: 1984.
- (42) Siegert, A. J. F. MIT Rad. Lab. Rep. no. 465, 1943.
- (43) Berne, B. J.; Pecora, R. *Dynamic Light Scattering*; John Wiley: New York, 1976.
- (44) Chu, B. *Laser Light Scattering*; Academic Press: New York, 1974.
- (45) Phillies, G. D. *J. Chem. Phys.* **1974**, *60*, 976.
- (46) Pusey, P. N.; Tough, R. J. A. In *Dynamic Light Scattering*; Pecora, R., Ed.; Plenum: New York, 1985; Chapter 4.
- (47) The relation obtained from the fluctuation theory cannot be applied to low salt ($<10^{-3}$ M) polyion solutions at *finite angles*, as shown by Vrij and Overbeek, because of the interference effects between different volume elements. However, the relation for 0° (eq 5) can still be applicable, because the necessary condition, $2 \sin(\theta/2)/(\kappa\lambda_0/n_0) \ll 1$, can be satisfied at 0° , where κ^{-1} is the Debye-Hückel screening length.⁴⁸
- (48) Vrij, A.; Overbeek, J. Th. G. *J. Colloid Sci.* **1962**, *17*, 570.
- (49) This relation may also be shown from the following relations: $D = D_0/S(q)^{50}$ and $R_\theta = KcMP(q)S(q)^{51}$ where $S(q)$ is the static structure factor. At $q = 0$, $D = D_0/S(0)$ and $R_0 = KcMS(0)$, and therefore $D \propto Kc/R_0$.
- (50) Ackerson, B. J. *J. Chem. Phys.* **1976**, *64*, 242.
- (51) Doty, P.; Steiner, R. F. *J. Chem. Phys.* **1952**, *20*, 85.
- (52) Brown, W., Ed. *Dynamic Light Scattering*; Clarendon Press: Oxford, U.K., 1993.
- (53) Oth, A.; Doty, P. *J. Phys. Chem.* **1952**, *56*, 43.
- (54) At extremely low concentrations, the $(1 - R_0/MKc)$ term in eq 8 is very close to zero and the real R_g values of polyion chains may be evaluated from the slope of q^2 -dependent curves.
- (55) Ise, N. *Angew. Chem., Int. Ed. Engl.* **1986**, *25*, 323.
- (56) Brown, W. *Polymer* **1984**, *25*, 680.
- (57) Brown, W.; Štěpánek, P. *Macromolecules* **1988**, *21*, 1791.
- (58) Ferrari, M. E.; Bloomfield, V. A. *Macromolecules* **1992**, *25*, 5266.
- (59) Drifford, M.; Dalbiez, J. P. *Biopolymers* **1985**, *24*, 1501.